

Published in final edited form as:

*Muscle Nerve*. 2013 April ; 47(4): 588–590. doi:10.1002/mus.23711.

## ARCHITECTURE OF HEALTHY AND DYSTROPHIC MUSCLES DETECTED BY OPTICAL COHERENCE TOMOGRAPHY

RICHARD M. LOVERING, PhD, PT<sup>1</sup>, SAMEER B. SHAH, PhD<sup>2</sup>, STEPHEN J.P. PRATT, BS<sup>1</sup>,  
WEI GONG, PhD<sup>3,4</sup>, and YU CHEN, PhD<sup>3</sup>

<sup>1</sup>University of Maryland School of Medicine, Department of Orthopaedics, 100 Penn Street, AHB, Room 540, Baltimore, Maryland, USA

<sup>2</sup>University of California, San Diego, Departments of Orthopaedic Surgery and Bioengineering, San Diego, California, USA

<sup>3</sup>University of Maryland, Fischell Department of Bioengineering, College Park, Maryland, USA

<sup>4</sup>Fujian Normal University, College of Photonic and Electronic Engineering, China

### Abstract

**Introduction**—The ability to view individual myofibers is possible with many histological techniques, but not yet with standard *in vivo* imaging. Optical coherence tomography (OCT) is an emerging technology that can generate high resolution 1–10  $\mu\text{m}$  cross-sectional imaging of tissue *in vivo* and in real time.

**Methods**—We used OCT to determine architectural differences of tibialis anterior muscles *in situ* from healthy mice (wild-type [WT],  $n = 4$ ) and dystrophic mice (*mdx*,  $n = 4$ ). After diffusion tensor imaging (DTI) and OCT, muscles were harvested, snap-frozen, and sectioned for staining with wheat germ agglutinin.

**Results**—DTI suggested differences in pennation and OCT was used to confirm this supposition. OCT indicated a shorter intramuscular tendon (WT/*mdx* ratio of 1.2) and an 18% higher degree of pennation in *mdx*. Staining confirmed these architectural changes.

**Conclusions**—Architectural changes in *mdx* muscles, which could contribute to reduction of force, are detectable with OCT.

### Keywords

*mdx*; mouse imaging; muscular dystrophy; skeletal muscle; small animal imaging

---

Muscle architecture refers to the macroscopic arrangement of myofibers within a muscle and their attachment to tendons at the myotendinous junction.<sup>1</sup> These properties have a significant effect on muscle function and muscle response to injury or disease.<sup>2</sup> Consequently, methods to characterize muscle architecture are important.

The muscular dystrophies are a heterogeneous group of inherited disorders characterized by progressive weakness and degeneration of skeletal muscles. Duchenne muscular dystrophy (DMD), the most common, is an X-linked disorder caused by the absence of dystrophin, a protein found on the cytoplasmic surface of the sarcolemma in striated muscle.<sup>3</sup> Dystrophin is also missing from *mdx* mice, an animal model for DMD.

This study compared the *in situ* architecture of healthy (wild-type, WT) and dystrophic (*mdx*) mouse skeletal muscle using optical coherence tomography (OCT). OCT provides a means to directly and rapidly assess architecture of muscles *in vivo*. OCT uses coherence gating of a light source to obtain images with extremely high spatial resolution, approaching the single micron level. OCT is an emerging tool that can provide real-time images of muscle *in situ*. OCT is able to image tissue (1–2 mm in depth) and generate three-dimensional images rapidly and without harmful effects to the tissue being studied.

## METHODS

### Animals

We used age-, strain-, and gender-matched 2- to 3-month-old male C57BL/10ScSn WT (n = 4) mice and *mdx* (n = 4) mice. Experimental procedures were approved by the University of Maryland Institutional Animal Care & Use Committee.

### Diffusion Tensor Imaging (DTI)

DTI was performed as described.<sup>4</sup> Imaging was performed using a Bruker Biospin (Billerica, Massachusetts) 7.0 Tesla MR system. Diffusion tensor reconstruction and tractography was performed (Fig. 1A) using Track-Vis (Massachusetts General Hospital; Boston, MA).

### Optical Coherence Tomography (OCT)

The WT and *mdx* mice used for DTI were allowed to recover from anesthesia, and several days later we examined the tibialis anterior (TA) muscles bilaterally on an OCT system previously described.<sup>5,6</sup> Mice were anesthetized, and the animal was placed in the supine position (Fig. 1B). To keep the muscles at comparable lengths, the ankles were maintained at 90° using a custom-designed splint. A small skin incision was made along the length of the TA for optimum scanning; the epimysium remained intact. The OCT system used a laser source that generates a broadband spectrum of ~100 nm full width at half maximum centered at 1,310 nm. A Michelson interferometer composed of a circulator and a fiber-optic 50/50 splitter was used to generate the Fourier-domain OCT interference signal. Virtual sections of reconstructed images from both TAs were examined to characterize muscle geometry and architecture. Fiber pennation angles were taken from the image slice used to obtain maximal internal tendon length (Fig. 1C). Curvature was calculated using the Straighten\_ jar plugin using ImageJ.<sup>7</sup>

### Histology

After OCT, the anesthetized animals were euthanized by perfusion with 4% paraformaldehyde in buffered saline while the ankles were maintained at 90°. The TAs were dissected,

and frozen muscle tissue was sectioned at 8  $\mu\text{m}$  in thickness and stained with Alexa Fluor 488 conjugated to wheat germ agglutinin (WGA).

## RESULTS

DTI provides a diffusion coefficient that is orientation-dependent for elongated structures such as myofibers.<sup>8,9</sup> DTI indicated an apparent change in fiber direction of the *mdx* mice compared with WT mice (Fig. 1A). When comparing WT and *mdx* TA cross-sections of whole mount unfrozen tissue (Fig. 1A), tendons are visible, however pennation angle is impossible to determine and finding a cut true to the maximal tendon length is difficult.

OCT was used to image TA muscles *in situ* (Fig. 1B). Images were searched to obtain maximal internal tendon length, fiber pennation angle, and overall shape of the TA muscle (Fig. 1C). The *mdx* muscles showed significant changes in all these parameters. The tendon length was shorter in *mdx* TAs ( $2.70 \pm 0.14$  mm) than in WT TAs ( $3.27 \pm 0.42$  mm;  $P < 0.05$ ). Fiber pennation angles were larger in *mdx* TAs ( $23 \pm 2^\circ$ ) compared with WT TAs ( $19 \pm 1^\circ$ ;  $P < 0.03$ ). These architectural differences were consistent with findings from the histological staining with WGA, where tendon length ( $2.61 \pm 0.2$  mm and  $3.14 \pm 0.27$  mm in the *mdx* and WT, respectively) was almost identical in proportion. The same was true for fiber pennation ( $24 \pm 3^\circ$  and  $19 \pm 2^\circ$  in the *mdx* and WT, respectively). Qualitatively, *mdx* muscles also appeared rounded, or swollen, compared with WT. Quantification of OCT images revealed a significantly higher maximum curvature for WT muscles compared with *mdx* ( $0.44 \pm 0.16$  mm<sup>-1</sup> vs.  $0.21 \pm 0.02$  mm<sup>-1</sup>;  $P < 0.03$ ).

## DISCUSSION

In this study, we describe the use of OCT to compare the architecture of TA muscles from normal and *mdx* mice, the latter still considered the most suitable mouse model for DMD.<sup>10</sup> OCT offers several advantages over other imaging modalities. Histology reveals that *mdx* skeletal muscle displays increased variability in myofiber size, malformed fibers, inflammation, and centrally located nuclei.<sup>11,12</sup> Although these findings are valuable, histology requires killing the animal, harvesting the tissue, and *ex vivo* study of muscle outside of its normal anatomical environment. Histology of muscle sections in different planes also requires the killing of additional animals for the added tissue needed to perform this task. Such tasks are labor-intensive and also create variability due to changes in tissue preservation or processing artifact.

DTI actually represents local muscle fiber directions in healthy rat TA muscle,<sup>13</sup> and Damon et al have used DTI fiber tracking to successfully measure pennation angles of myofibers in human skeletal muscle.<sup>9,14-16</sup> However, DTI relies on anisotropic flow of water along the long axis of intact myofibers<sup>8,9</sup> and thus cannot reliably assess architecture in dystrophic muscle.

OCT allows one to directly visualize the internal architecture of a muscle. Our application of *in vivo* OCT to examine muscle architecture builds on the previous use of OCT in mice to examine exercise-induced damage,<sup>17</sup> evaluation of muscle autografts,<sup>18</sup> and even to identify necrotic muscle tissue in *mdx* mice.<sup>19</sup> We examined TA muscles, and the results indicated a

shorter intramuscular tendon and a higher degree of pennation in *mdx*. Future studies could relate changes in architecture to changes in joint position, with aging or after damage.

## Acknowledgments

This work was supported by grants to RML from the National Institutes of Health (K01AR053235 and 1R01AR059179).

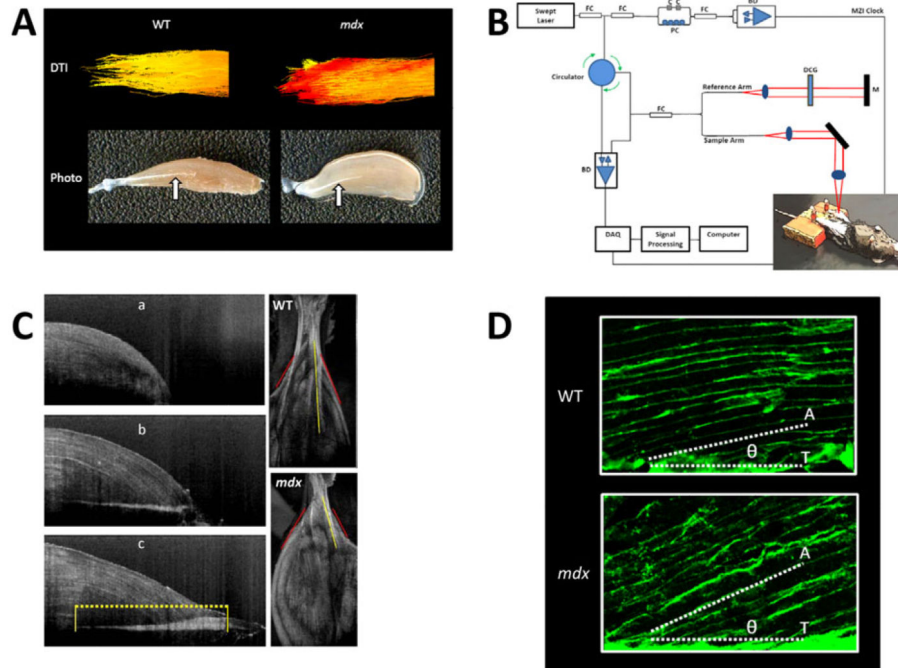
## Abbreviations

<b>DMD</b>	Duchenne muscular dystrophy
<b>DTI</b>	diffusion tensor imaging
<b>OCT</b>	optical coherence tomography
<b>TA</b>	tibialis anterior
<b>WGA</b>	wheat germ agglutinin
<b>WT</b>	wild-type

## REFERENCES

1. Gans C, Bock WJ. The functional significance of muscle architecture—a theoretical analysis. *Ergeb Anat Entwicklungsgesch.* 1965; 38:115–142. [PubMed: 5319094]
2. Lieber RL, Friden J. Functional and clinical significance of skeletal muscle architecture. *Muscle Nerve.* 2000; 23:1647–1666. [PubMed: 11054744]
3. Duchenne, G. *l'Electrisation Localisee et de son Application a la Pathologie et a la Therapeutique* Paris. Bailliere et Fils: Bailliere et Fils; 1861.
4. McMillan AB, Shi D, Pratt SJ, Lovering RM. Diffusion tensor MRI to assess damage in healthy and dystrophic skeletal muscle after lengthening contractions. *J Biomed Biotechnol.* 2011; 2011:970726. [PubMed: 22190860]
5. Yuan S, Roney CA, Wierwille J, Chen CW, Xu B, Griffiths G, et al. Co-registered optical coherence tomography and fluorescence molecular imaging for simultaneous morphological and molecular imaging. *Phys Med Biol.* 2010; 55:191–206. [PubMed: 20009192]
6. Yuan S, Li Q, Jiang J, Cable A, Chen Y. Three-dimensional coregistered optical coherence tomography and line-scanning fluorescence laminar optical tomography. *Opt Lett.* 2009; 34:1615–1617. [PubMed: 19488125]
7. Kocsis E, Trus BL, Steer CJ, Bisher ME, Steven AC. Image averaging of flexible fibrous macromolecules: the clathrin triskelion has an elastic proximal segment. *J Struct Biol.* 1991; 107:6–14. [PubMed: 1817611]
8. Heemskerk AM, Strijkers GJ, Vilanova A, Drost MR, Nicolay K. Determination of mouse skeletal muscle architecture using three-dimensional diffusion tensor imaging. *Magn Reson Med.* 2005; 53:1333–1340. [PubMed: 15906281]
9. Heemskerk AM, Sinha TK, Wilson KJ, Ding Z, Damon BM. Quantitative assessment of DTI-based muscle fiber tracking and optimal tracking parameters. *Magn Reson Med.* 2009; 61:467–472. [PubMed: 19161166]
10. Willmann R, Possekel S, Dubach-Powell J, Meier T, Ruegg MA. Mammalian animal models for Duchenne muscular dystrophy. *Neuromuscul Disord.* 2009; 19:241–249. [PubMed: 19217290]
11. Li ZB, Zhang J, Wagner KR. Inhibiting myostatin reverses muscle fibrosis through apoptosis. *J Cell Sci.* 2012 Epub ahead of print.
12. Chamberlain JS, Metzger J, Reyes M, Townsend D, Faulkner JA. Dystrophin-deficient *mdx* mice display a reduced life span and are susceptible to spontaneous rhabdomyosarcoma. *FASEB J.* 2007; 21:2195–2204. [PubMed: 17360850]

13. Van Donkelaar CC, Kretzers LJ, Bovendeerd PH, Lataster LM, Nicolay K, Janssen JD, et al. Diffusion tensor imaging in biomechanical studies of skeletal muscle function. *J Anat.* 1999; 194(Pt 1):79–88. [PubMed: 10227669]
14. Damon BM, Ding Z, Anderson AW, Freyer AS, Gore JC. Validation of diffusion tensor MRI-based muscle fiber tracking. *Magn Reson Med.* 2002; 48:97–104. [PubMed: 12111936]
15. Kan JH, Heemskerk AM, Ding Z, Gregory A, Mencia G, Spindler K, et al. DTI-based muscle fiber tracking of the quadriceps mechanism in lateral patellar dislocation. *J Magn Reson Imaging.* 2009; 29:663–670. [PubMed: 19243049]
16. Lansdown DA, Ding Z, Wadlington M, Hornberger JL, Damon BM. Quantitative diffusion tensor MRI-based fiber tracking of human skeletal muscle. *J Appl Physiol.* 2007; 103:673–681. [PubMed: 17446411]
17. Pasquesi JJ, Schlachter SC, Boppart MD, Chaney E, Kaufman SJ, Boppart SA. In vivo detection of exercised-induced ultrastructural changes in genetically-altered murine skeletal muscle using polarization-sensitive optical coherence tomography. *Opt Express.* 2006; 14:1547–1556. [PubMed: 19503481]
18. Klyen BR, Armstrong JJ, Adie SG, Radley HG, Grounds MD, Sampson DD. Three-dimensional optical coherence tomography of whole-muscle autografts as a precursor to morphological assessment of muscular dystrophy in mice. *J Biomed Opt.* 2008; 13:011003. [PubMed: 18315352]
19. Klyen BR, Shavlakadze T, Radley-Crabb HG, Grounds MD, Sampson DD. Identification of muscle necrosis in the mdx mouse model of Duchenne muscular dystrophy using three-dimensional optical coherence tomography. *J Biomed Opt.* 2011; 16:076013. [PubMed: 21806274]

**FIGURE 1.**

(A) Indications of differences in gross morphology. Top panels show examples of “fiber tracking” from processed DTI. The image shows modeling of fiber tracks in TA muscles of a control (WT) mouse and a dystrophic (*mdx*) mouse where yellow indicates anisotropic flow, or a more “linear” fiber, and red indicates more isotropy. Bottom panels of 1A show photographs of harvested muscles filleted open. (B) Schematic of the OCT imaging system. The animal was anesthetized, and the lower extremities were positioned using a custom-designed device. FC, fiber coupler; PC, polarization controller; C, collimator; MZI, Mach-Zehnder interferometer; M, mirror; BD, balanced detector; DAQ, data acquisition board; DCG, dispersion compensating glasses; OBJ, objective. (C) Left (a–c): Z-stack OCT images of the mouse TA were surveyed to find maximal tendon length (dotted yellow line) and measure pennation angle. Right: Measurements were made of the overall shape of the distal TA muscle (outside angle, red line) as it arose from the tendon (solid yellow line). (D) WGA was used to stain sections for histological assessment of myofiber pennation (U). Myofibers are oriented somewhat parallel to the force-generating axis along the tendon (T) or at angles relative to the force-generating axis (A).